Two Adaptive Space - Time Block Coded MIMO Systems Exploiting Partial Channel Knowledge at the Transmitter

Gerhard Gritsch, Gerald Kolar, Hans Weinrichter, Markus Rupp

Institute for Communications and Radio Frequency Engineering, Vienna University of Technology
Gusshausstr. 25, A-1040 Vienna, Austria
e-mail: (ggritsch,gkolar,jweinri,mrupp)@nt.tuwien.ac.at

Abstract

In this contribution two new closed loop transmission schemes over wireless MIMO channels with only partial channel knowledge at the transmitter are presented. Utilizing Space Time Block Codes (STBCs) with additional pre- and post signal processing provides n_T independent virtual channels, where n_T is the number of transmit antennas. In most cases we consider $n_T = 4$. The first scheme is based on the Extended Alamouti (EA) code, transmitting R=1 information symbol per channel use. This scheme requires only a very low feedback rate. The second scheme achieves a higher rate of R=2 information symbols per channel use, but it needs more feedback information. This high rate data transmission is achieved by utilizing the Double Space Time Transmit Diversity (D-STTD) code. The modulation format (from 2PSK to 256QAM) used on the resulting n_T independent virtual channels is adapted to the individual quality of the virtual channels. For a given target Bit Error Ratio (BER) and a fixed mean transmit power an adaptive algorithm maximizes the data throughput. With these two closed loop schemes very high data rates at reasonably low values of SNR are achieved. Simulation results show that the first scheme is very robust against spatial correlation with respect to the mean information bit rate.

1 Introduction

Recent research in the field of closed loop transmission schemes over wireless MIMO channels shows that some feedback information about the channel state is a proper mean to improve the system performance. Various transmission schemes use only partial feedback information to improve the BER-performance, e.g. [5]. Other approaches aim to achieve very high data rate [7], but need a large amount of feedback information. It is clear that there is a tradeoff between performance, information rate and feedback rate for such Closed Loop Schemes (CLSs).

The proposed schemes diagonalize the MIMO channel matrix with the aid of STBCs and use some additional pre- and post signal processing. At the input of the resulting n_T virtual channels, adaptive modulation is used to exploit the maximum possible information rate for a given SNR.

Our first scheme uses the Extended Alamouti (EA) code [4]. The corresponding data rate is $R = 1$ symbol per channel use and only a very low feedback information rate is required. The second scheme utilizes the so called Double Space Time Transmit Diversity (D-STTD) code introduced in [3]. The price to be paid for the higher information rate ($R = 2$ symbols per channel use) of the D-STTD compared to the EA is the need of a considerably higher rate of feedback information.

The rest of the paper is organized as follows. Sec. 2 deals with the used channel model. Sec. 3 is devoted to the scheme which uses the EA code. Sec. 4 explains the diagonalization of the virtual channel matrix with the aid of the D-STTD code. Essential results are summarized in the last chapter.

2 Channel Model

In this paper the behavior of the channel in the time domain is assumed as a temporally uncorrelated block Rayleigh fading, i.e., the channel is constant during the block length of the STBC and afterwards changes independently. The time interval when the channel is assumed to be constant depends on the used transmission scheme. For the scheme utilizing the EA code, the channel is constant for n_T symbol durations. For the D-STTD scheme the channel is assumed to be constant for two symbol durations. In simulations spatially uncorrelated and spatially correlated fading channels are investigated.

2.1 Spatially Uncorrelated Channel

In the case of spatially uncorrelated fading the simple IID (Independent, Identically Distributed) Rayleigh fading channel model is used. For this IID channel model the entries of the channel matrix $\mathbf{H}$ are independent complex Gaussian distributed random variables with zero mean and unit variance:

$$\mathbf{H} \sim \mathcal{N}_C^{n_R \times n_T}$$

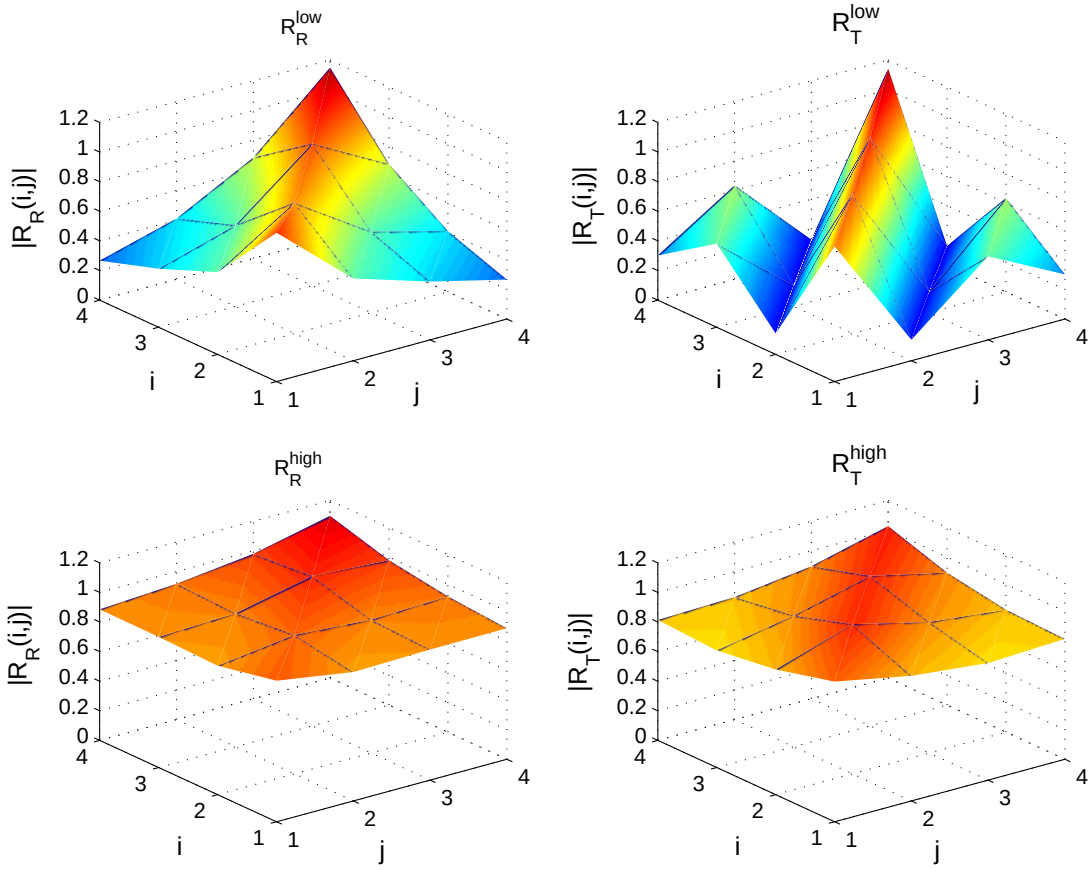

Fig. 1. The upper left figure shows the magnitude of the entries of the receiver correlation matrix for low spatial correlation $\mathbf{R}_{\mathrm{R}}^{\mathrm{low}}$. i and j denotes the i-th row and the j-th column of the corresponding correlation matrix. The upper right figure shows the magnitude of the entries of the transmitter correlation matrix for low spatial correlation $\mathbf{R}_{\mathrm{T}}^{\mathrm{low}}$. The lower left figure shows the magnitude of the entries of the receiver correlation matrix for high spatial correlation $\mathbf{R}_{\mathrm{R}}^{\mathrm{high}}$. The lower right figure shows the magnitude of the entries of the transmitter correlation matrix for high spatial correlation $\mathbf{R}_{\mathrm{T}}^{\mathrm{high}}$.

2.2 Spatially Correlated Channel

For the spatially correlated case, the well known Kronecker model is used [1],[2]. For this model a transmit correlation matrix $\mathbf{R}_T$, a receive correlation matrix $\mathbf{R}_R$ and an IID complex Gaussian matrix $\mathbf{G} \in \mathcal{N}_C^{n_R \times n_T}$ is used to model the fading channel:

$$\mathbf{H} = \mathbf{R}_R^{1/2}\, \mathbf{G}\, \left(\mathbf{R}_T^{1/2}\right)^T . \qquad (1)$$

The correlation matrices $\mathbf{R}_R = E_{\mathbf{H}}\left\{\mathbf{H}\mathbf{H}^H\right\}$ and $\mathbf{R}_T = E_{\mathbf{H}}\left\{\mathbf{H}^H\mathbf{H}\right\}$ are normalized in such a way, that $E_{\mathbf{H}}\left(\mathrm{tr}\left(\mathbf{H}^H\mathbf{H}\right)\right) = n_R\, n_T$, as in the IID case.

The correlation matrices were extracted from MIMO channel measurements, which have been specified in [6]. At the transmitter and at the receiver uniform linear antenna arrays have been used. For the simulations two different pairs of correlation matrices are used. High spatial correlation is modeled by the following pair of correlation matrices:

$$\mathbf{R}_{\mathrm{R}}^{\mathrm{high}} = \begin{pmatrix} 0.953-j0.000 & 0.015-j0.870 & -0.879-j0.071 & -0.079+j0.882 \\ 0.015+j0.870 & 0.939-j0.000 & 0.023-j0.901 & -0.915-j0.073 \\ -0.879-j0.071 & 0.023-j0.901 & 1.013-j0.000 & 0.009-j0.979 \\ -0.079+j0.882 & -0.915-j0.073 & 0.009-j0.979 & 1.096+j0.000 \end{pmatrix}$$

$$\mathbf{R}_{\mathrm{T}}^{\mathrm{high}} = \begin{pmatrix} 0.947-j0.000 & -0.093-j0.841 & -0.783+j0.113 & 0.233+j0.780 \\ -0.093+j0.841 & 1.011-j0.000 & -0.131-j0.876 & -0.809+j0.176 \\ -0.783-j0.113 & -0.131+j0.876 & 1.015-j0.000 & -0.152-j0.883 \\ 0.233-j0.780 & -0.809-j0.176 & -0.152+j0.883 & 1.027+j0.000 \end{pmatrix}$$

Low spatial correlation is modeled by:

$$\mathbf{R}_{\mathrm{R}}^{\mathrm{low}} = \begin{pmatrix} 1.005-j0.000 & 0.212-j0.512 & -0.382-j0.099 & 0.034+j0.264 \\ 0.212+j0.512 & 0.884-j0.000 & 0.254-j0.487 & -0.391-j0.128 \\ -0.382+j0.099 & 0.254+j0.487 & 0.961-j0.000 & 0.302-j0.610 \\ 0.034-j0.264 & -0.391+j0.128 & 0.302+j0.610 & 1.149+j0.000 \end{pmatrix}$$

$$\mathbf{R}_{\mathrm{T}}^{\mathrm{low}} = \begin{pmatrix} 0.912-j0.000 & 0.098-j0.102 & -0.191-j0.531 & -0.274-j0.128 \\ 0.098+j0.102 & 0.943-j0.000 & 0.086-j0.114 & -0.269-j0.576 \\ -0.191+j0.531 & 0.086+j0.114 & 1.002-j0.000 & 0.098-j0.081 \\ -0.274+j0.128 & -0.269+j0.576 & 0.098+j0.081 & 1.143+j0.000 \end{pmatrix}$$

Note that the matrices $\mathbf{R}_{\mathrm{R}}^{\mathrm{high}}$ and $\mathbf{R}_{\mathrm{T}}^{\mathrm{high}}$ for the high spatial correlation case correspond to the measurement scenario 13D1 and the matrices $\mathbf{R}_{\mathrm{R}}^{\mathrm{low}}$ and $\mathbf{R}_{\mathrm{T}}^{\mathrm{low}}$ for the low spatial correlation case correspond to the measurement scenario 24D3 in [6]. In order to give the reader a flavor of the corresponding spatial correlations for these two scenarios, the magnitudes of the entries of the correlation matrices for low and high spatial correlation at the transmitter and at the receiver side are plotted in Fig. 1. Of course, the correlation values shown in Fig. 1, 5 and 8 are only valid for integer values of i and j. This is due to the definition of the correlation values between the corresponding antenna elements with integer labels i and j.

3 Extended Alamouti Scheme

As mentioned in Sec. 1, the scheme with low feedback rate utilizes the EA codes for the diagonalization of the MIMO channel matrix. These codes exist for $n_T = 2^k$ with $k = 2, 3, 4, \ldots$. The number of receive antennas n_R can be chosen arbitrarily. In the following, the scheme with $n_T = 4$ is investigated, but matters are quite similar for $n_T = 2^k$.

3.1 Diagonalization Principle

Note that the EA has a recursive Hadamard type structure, i.e., the code matrix for the $n_T = 4$ scheme can be constructed by four Alamouti type (2×2) code matrices. More details about the construction method are provided in [4]. The EA code for $n_T = 4$ results in:

$$\mathbf{S} = \begin{bmatrix} s_1 & s_2 & s_3 & s_4 \\ s_2^* & -s_1^* & s_4^* & -s_3^* \\ s_3^* & s_4^* & -s_1^* & -s_2^* \\ s_4 & -s_3 & -s_2 & s_1 \end{bmatrix} \tag{2}$$

In the following section, the channel diagonalization is shown for the special case of $n_R = 1$. This method is generalized to other values of n_R in Sec. 3.1.2.

3.1.1 Special Case: $n_R = 1$

The code matrix $\mathbf{S}$ is transmitted via the MISO channel with transmit vector $\mathbf{h} = (h_{11}\, h_{12}\, h_{13}\, h_{14})$. Gaussian noise $\mathbf{n}$ is added at the receiver input. We assume that the channel is constant for the 4 symbol intervals of the code block. The received signal $\mathbf{y}$ results in:

$$\mathbf{y} = \mathbf{h}\,\mathbf{S}^T + \mathbf{n}\,, \tag{3}$$

with $\mathbf{y} = [y_1\ y_2\ y_3\ y_4]$. A mathematically equivalent description of (3) is:

$$\tilde{\mathbf{y}} = \mathbf{H}_v\,\mathbf{s} + \tilde{\mathbf{n}}\,, \tag{4}$$

where $\tilde{\mathbf{y}} = [y_1\ y_2^*\ y_3^*\ y_4]^T$, $\mathbf{s} = [s_1\ s_2\ s_3\ s_4]^T$ and the resulting virtual channel matrix $\mathbf{H}_v$ is:

$$\mathbf{H}_v = \begin{bmatrix} h_{11} & h_{12} & h_{13} & h_{14} \\ -h_{12}^* & h_{11}^* & -h_{14}^* & h_{13}^* \\ -h_{13}^* & -h_{14}^* & h_{11}^* & h_{12}^* \\ h_{14} & -h_{13} & -h_{12} & h_{11} \end{bmatrix} \tag{5}$$

At the receiver $\tilde{\mathbf{y}}$ is processed by a "matched filter" $\mathbf{H}_v^H$ resulting in the modified receive vector

$$\tilde{\mathbf{y}}_{mod} = \mathbf{H}_v^H \mathbf{H}_v \mathbf{s} + \mathbf{H}_v^H \mathbf{n}\,. \tag{6}$$

The essential advantage of the EA code as described in (2) is that the resulting Grammian matrix $\mathbf{G}_v = \mathbf{H}_v^H \mathbf{H}_v$ in (6) can be diagonalized by a unitary matrix $\mathbf{V}$ that is independent from the actual channel vector $\mathbf{h}$:

$$\mathbf{V} = \frac{1}{\sqrt{2}} \begin{bmatrix} 0 & 1 & 0 & -1 \\ -1 & 0 & 1 & 0 \\ 1 & 0 & 1 & 0 \\ 0 & 1 & 0 & 1 \end{bmatrix} \tag{7}$$

This is true because of the specific structure of the virtual channel matrix $\mathbf{H}_v$ shown in (5). Diagonalizing $\mathbf{G}_v$ we obtain the diagonal matrix $\mathbf{D} = \mathrm{diag}(\lambda_1, \lambda_2, \ldots \lambda_4)$ as

$$\mathbf{D} = \mathbf{V}^H\, \mathbf{H}_v^H\, \mathbf{H}_v\, \mathbf{V}\,. \tag{8}$$

Applying this diagonalization we can easily transform our EA coded transmission scheme into $n_T = 4$ independent virtual channels with distinct channel gains λ_i, $i = 1, 2, \ldots, 4$. This is done by pre-processing our transmit signal vector $\mathbf{s}$ by the Eigenmatrix $\mathbf{V}$ and by the post-processing the modified receive vector $\tilde{\mathbf{y}}_{mod}$ by $\mathbf{V}^H$. In this way we get n_T decoupled scaled estimates $\hat{\mathbf{s}}$ of $\mathbf{s}$:

$$\hat{\mathbf{s}} = \mathbf{V}^H\, \mathbf{H}_v^H\, \mathbf{H}_v\, \mathbf{V}\mathbf{s} + \mathbf{V}^H\, \mathbf{H}_v^H\, \tilde{\mathbf{n}} = \mathbf{D}\mathbf{s} + \mathbf{n}_m\,. \tag{9}$$

The $n_T = 4$ channel gains λ_i, which are the Eigenvalues of the diagonal matrix $\mathbf{D}$, can be evaluated as

$$\lambda_1 = \lambda_2 = h(1 + X) \qquad \lambda_3 = \lambda_4 = h(1 - X) \tag{10}$$

with

$$X = 2Re\left\{h_{11}h_{14}^* - h_{12}h_{13}^*\right\}/h \tag{11}$$

$$h = |h_{11}|^2 + |h_{12}|^2 + |h_{13}|^2 + |h_{14}|^2. \tag{12}$$

Note that the modified noise $\mathbf{n}_m$ is still uncorrelated:

$$\mathbf{R}_{\mathbf{n}_m} = E_{\mathbf{n}}(\mathbf{n}_m\, \mathbf{n}_m^H) = E_{\mathbf{n}}(\mathbf{V}^H \mathbf{H}_v^H \tilde{\mathbf{n}}\, \tilde{\mathbf{n}}^H\, \mathbf{H}_v\, \mathbf{V}) = \mathbf{D}\,\sigma_n^2$$

3.1.2 Other values of n_R

The method just described can be generalized for arbitrary values of n_R. The virtual matrix channel $\mathbf{H}_v$ becomes an $(n_R \cdot n_T) \times n_T$ matrix, but the resulting Grammian matrix $\mathbf{G}_v = \mathbf{H}_v^H \mathbf{H}_v$ again has the same structure as above and therefore the same channel independent unitary matrix $\mathbf{V}$ can be used for the pre- and post signal processing of $\mathbf{s}$. The channel gains are calculated as above, but the entities h and X now result in:

$$X = \frac{1}{h} \sum_{i=1}^{n_R} h^{(i)} X^{(i)} \tag{13}$$

$$h = \sum_{i=1}^{n_R} h^{(i)} \tag{14}$$

for i=1, 2, ..., n_R with

$$X^{(i)} = 2Re\left\{h_{i1}h_{i4}^* - h_{i2}h_{i3}^*\right\}/h^{(i)} \tag{15}$$

$$h^{(i)} = |h_{i1}|^2 + |h_{i2}|^2 + |h_{i3}|^2 + |h_{i4}|^2. \tag{16}$$

The fundamental advantage of this coding scheme is that no feedback information about the actual channel is necessary to diagonalize the MIMO channel matrix!

3.2 Adaptive Modulation

Having diagonalized the Grammian matrix $\mathbf{G}_v$, n_T independent virtual channels of different quality (different values of SNR due to the distinct Eigenvalues λ_i) are obtained. The modulation format used at each virtual channel is adapted to its actual quality (measured in terms of SNR). The set of possible modulation formats used ranges from 2PSK to 256QAM [8].

An adaptive algorithm maximizes the throughput under the constraints of a fixed mean transmit power and a fixed target Bit Error Ratio $\text{BER}_{\text{target}}$.

The BER of the eight different modulation schemes can be calculated with eight different equations, which all have the same structure:

$$\text{BER}_i \sim \alpha_i \, Q(\sqrt{\beta_i \, \lambda_j \, \text{SNR}}) \, , \qquad (17)$$

where $Q(.)$ denotes the Marcum Q-function. The individual BERs mainly depend on the channel gains λ_j of the n_T virtual channels and on the mean SNR. The constants α_i and β_i depend on the specific modulation format [8]. If the BER in (17) is set to $\text{BER}_{\text{target}}$ and the mean SNR is known, then the thresholds λ_k^t of the channel gains for which the considered modulation scheme achieves a BER which is equal to $\text{BER}_{\text{target}}$ can be calculated. In Fig. 2 the thresholds λ_k^t are shown as a function of the mean SNR for a $\text{BER}_{\text{target}} = 10^{-3}$ for modulation formats from 2PSK to 256QAM. The

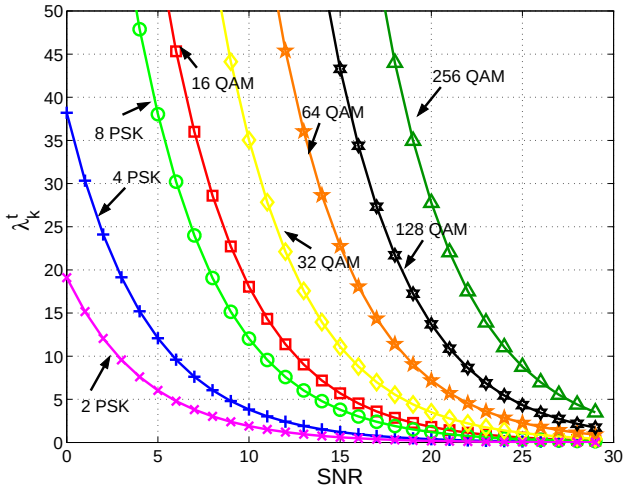

Fig. 2. Thresholds λ_k^t of the channel gains for $\text{BER}_{\text{target}} = 10^{-3}$ as a function of the mean SNR for modulation formats from 2PSK to 256QAM.

adaptation algorithm relies on the thresholds λ_k^t for all modulation schemes (2PSK to 256QAM) given in Fig. 2 and on the knowledge of the mean SNR. With the measured channel gains λ_i and the thresholds λ_k^t a proper modulation format for each virtual channel can be selected. For example, if $\lambda_i > \lambda_{16\text{QAM}}^t$ and $\lambda_i < \lambda_{32\text{QAM}}^t$, then 16QAM is used at the i-th virtual channel. If a channel gain λ_i is smaller then the threshold $\lambda_{2\text{PSK}}^t$ for 2PSK, then this virtual channel is not used at all.

As mentioned in Sec. 3.1, no feedback information is necessary for the diagonalization of the virtual channel matrix, but some feedback is needed for the selection of the modulation format. We assume that the receiver has full channel knowledge. The receiver determines the best fitting modulation format for each virtual channel and informs the transmitter, which modulation schemes should be used on each virtual channel. Remember (10), which shows that there are two pairs of two identical virtual channels and therefore the adaptation of the modulation must be done only for two distinct channel gains. Because of the option of eight distinct modulation formats and no transmission at all in case of very low channel gain, four feedback bits are necessary to control the modulation format at each virtual channel. Therefore the total number of feedback bits is $2 \times 4 = 8$ bits per fading block.

In the case of a slowly varying environment, one can think of switching into a quasi static feedback mode, where only one feedback bit is used for each of the different virtual channels. Only if the adaptation of the modulation is necessary due to a change of the channel state, then one bit for each different virtual channel is sent back to inform the transmitter which modulation scheme should be used now: one step above the current modulation or one step below the current modulation. In this mode, many feedback bits can be saved.

In the upper part of Fig. 3 the main processing blocks of the proposed transceiver are shown. Note that the dashed lines in the *adaptive modulation* block and in the *slicer* block indicate that the adaptive modulation and the symbol detection is performed for each virtual channel separately. Due to the decoupled signal streams, the complexity of Maximum Likelihood (ML) detection is very low.

In the lower part of Fig. 3 the mathematically equivalent description of the whole signal processing performed in the upper part of Fig. 3 is shown. In fact, with the aid of the EA code the transmit system is decomposed into the adaptive modulation of four independent virtual channels with distinct gains λ_i.

3.3 Simulation Results

Simulations have been performed for MIMO channels with $n_T = n_R = 4$ and different values of mean SNR. The mean SNR is defined as:

$$\text{SNR} = \frac{n_T P_s}{\sigma_n^2} = \frac{4}{\sigma_n^2}, \qquad (18)$$

where P_s and σ_n^2 are the mean transmit power per antenna and the receiver noise power at each receive antenna. All modulation formats used are normalized to $P_s = 1$ and therefore the right hand side in (18) holds. Different spatially correlated MIMO channels have been simulated. As mentioned in Sec. 2, we have investigated three different spatially correlated channel types (uncorrelated, low correlation and high correlation). Note that the simulations have been performed

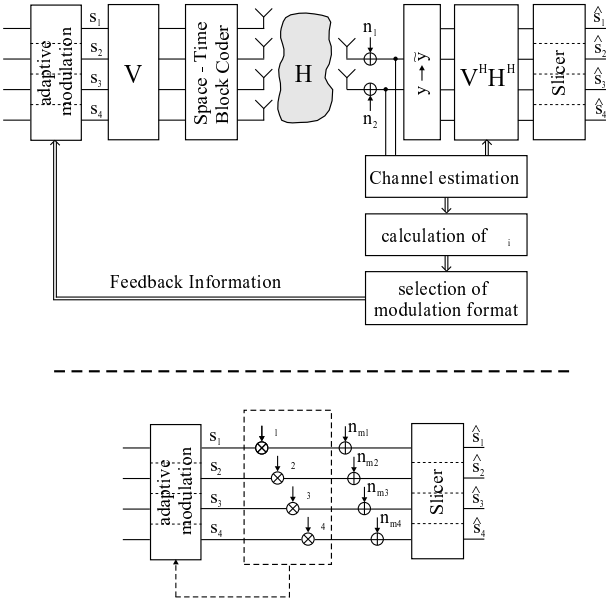

Fig. 3. The upper part of the figure shows the main processing blocks of the proposed transceiver with four transmit and two receive antennas. The lower part shows the equivalent mathematical description of the whole system.

assuming perfect channel knowledge at the receiver and error free transmission of the feedback information. Delay effects of feedback data are neglected.

The desired mean BER $= 10^{-3}$ has been chosen. As explained above, the adaptation algorithm chooses modulation schemes, which always achieve BERs that are less or equal to this $\text{BER}_{\text{target}}$ and therefore the resulting mean BER is in fact less the 10^{-3}. For this reason the $\text{BER}_{\text{target}}$ can be slightly increased, so that at last the resulting mean BER is in fact equal to 10^{-3}.

3.3.1 Mean rate $\overline{R}$

In Fig. 4, the mean information bit rates $\overline{R}$ versus the mean SNR are shown for a mean BER of 10^{-3} and three different spatial correlations. The surprising result is that the mean performance of this scheme is extremely robust against spatial channel correlation. Note that the spatial correlation is extremely high in the case of "high correlation" (Fig. 1). The increase in data rate $\overline{R}$ with increasing SNR is approximately 3.5 bit / 10dB SNR for all channel types.

An explanation for the robustness of our scheme with respect to spatial correlation is that the EA code achieves a very good decorrelation of the channel. Our scheme is based on the virtual channel matrix $\mathbf{H}_v = [\mathbf{h}_{v_1}\ \mathbf{h}_{v_2} \dots\ \mathbf{h}_{v_{n_T}}]$. The transmitter correlation $\mathbf{R}_T^v = E_{\mathbf{H}}\left\{\mathbf{H}_v^H \mathbf{H}_v\right\}$ of this virtual matrix $\mathbf{H}_v$ (depicted in Fig. 5) shows that the correlation for $i \neq j$ is by far not as high as for the real channel matrix $\mathbf{H}$ (lower right part of Fig. 1) and therefore nearly no degradation in the mean bit rate is observed compared to a transmission over an uncorrelated channel. Note that due to the special structure of $\mathbf{H}_v^H \mathbf{H}_v$, the virtual correlation matrix $\mathbf{R}_T^v$ has only non zero values on the main diagonal and the anti diagonal (i,j: 1,4 | 2,3 | 3,2 | 4,1).

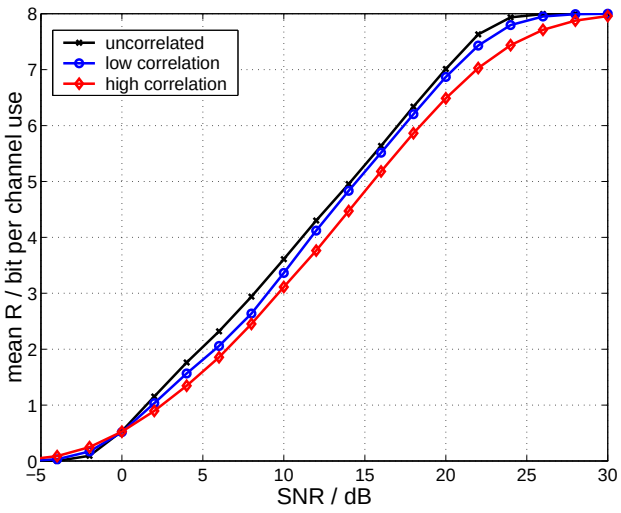

Fig. 4. Mean information bit rate $\overline{R}$ versus the mean SNR for several spatial correlation conditions (uncorrelated, low-, high-correlation) for a mean BER of 10^{-3}; EA scheme; $n_T = n_R = 4$.

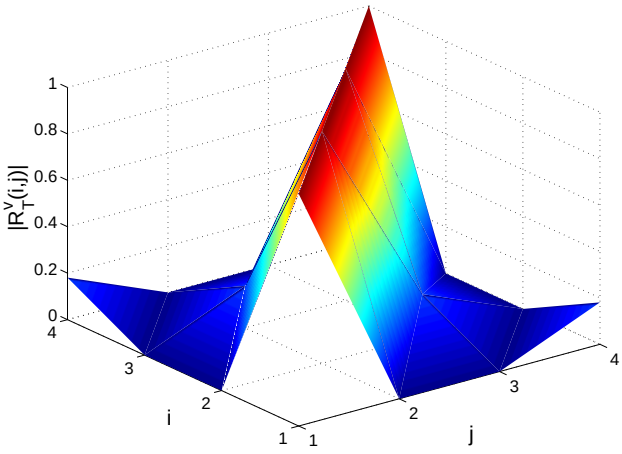

Fig. 5. Transmitter correlation $\mathbf{R}_T^v(i,j) = E_{\mathbf{H}}\left\{\mathbf{h}_{v_i}^H \mathbf{h}_{v_j}\right\}$ of the virtual channel matrix $\mathbf{H}_v = [\mathbf{h}_{v_1}\ \mathbf{h}_{v_2} \dots\ \mathbf{h}_{v_{n_T}}]$ for the EA scheme with $n_R = n_T = 4$ in case of "high spatial correlation".

3.3.2 Outage rate R_{out}

In Fig. 6, the Cumulative Distribution Functions (CDFs) of the rate R are shown for SNR=14dB and a mean BER of 10^{-3} and three spatial correlations. As can be seen, the proposed system is quite sensitive on spatial correlation with respect to outage rate. For example, considering an outage probability of 10%, the rates for uncorrelated, low correlated and high correlated channels are $R_{out}^{10\%}$=4.1, 3.7 and 2.5 bit per channel use. In fact the spatial correlation leads to an increased variation of the achievable rate. Thus, the 10% outage rate decreases substantially with increasing spatial correlation, although the mean rate remains almost unaffected from spatial correlation.

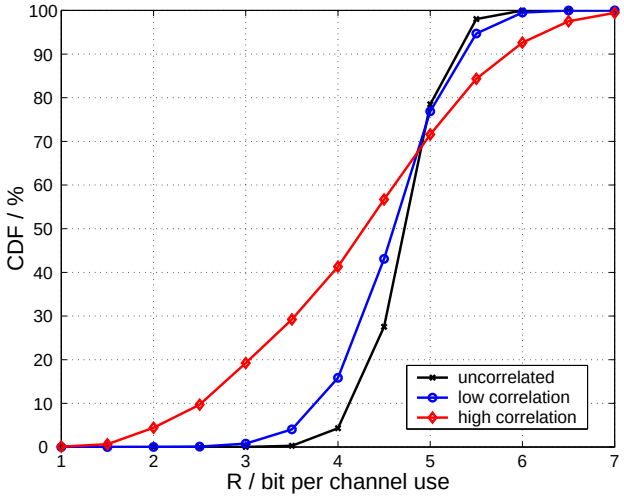

Fig. 6. CDFs of rate R for SNR=14dB and several spatial correlation conditions (uncorrelated, low-, high-correlation) for a mean BER of 10^{-3}; EA scheme; $n_T = n_R = 4$.

4 D-STTD Scheme

As mentioned in Sec. 1, the high rate scheme with moderate feedback rate utilizes the D-STTD code for MIMO channel diagonalization. Such codes exist for $n_T = 2\,k$ with $k = 2, 3, 4, \ldots$. In fact, only for the code with $k = 2$ the name double STTD is really justified. Again the Grammian matrix $\mathbf{G}_v = \mathbf{H}_v^H \mathbf{H}_v$ of the corresponding virtual channel matrix has a specific structure. Accordingly, the diagonalization matrix $\mathbf{V}$ (defined in (24)) has a specific structure too for any value of n_R. If the number of receive antennas is chosen to be $n_R \geq n_T/2$, then the maximum number n_T of independent virtual channels is obtained. Using fewer receive antennas, a smaller number of independent virtual channels is achieved. In the following the scheme with $n_T = 4$ is investigated, but matters are quite similar for other even valued numbers of n_T.

4.1 Diagonalization Principle

The D-STTD Code (again generalized from the (2×2) Alamouti scheme) for $n_T = 4$ is defined as:

$$\mathbf{S} = \begin{pmatrix} s_1 & s_2 & s_3 & s_4 \\ -s_2^* & s_1^* & -s_4^* & s_3^* \end{pmatrix} . \tag{19}$$

That means, we transmit four symbols over four transmit antennas in two time slots. In the following, the channel diagonalization is shown for the special case of $n_R = 2$. The extension to general values of n_R is explained in Sec. 4.1.2.

4.1.1 Special Case: $n_R = 2$

The code matrix $\mathbf{S}$ is transmitted via the real MIMO channel described by the transfer matrix

$$\mathbf{h} = \begin{pmatrix} h_{11} & h_{12} & h_{13} & h_{14} \\ h_{21} & h_{22} & h_{23} & h_{24} \end{pmatrix} . \tag{20}$$

Gaussian noise is added at each receiver input. The channel is assumed to be constant for two symbol durations. Then, the received signal $\mathbf{y}$ is:

$$\mathbf{y} = \begin{pmatrix} y_{11} & y_{12} \\ y_{21} & y_{22} \end{pmatrix} = \mathbf{h}\,\mathbf{S}^T + \mathbf{n}\,. \tag{21}$$

A mathematically equivalent description is:

$$\tilde{\mathbf{y}} = \mathbf{H}_v\,\mathbf{s} + \tilde{\mathbf{n}}\,, \tag{22}$$

where $\tilde{\mathbf{y}} = [y_{11}\ y_{12}^*\ y_{21}\ y_{22}^*]^T$, $\mathbf{s} = [s_1\ s_2\ s_3\ s_4]^T$ and the resulting virtual channel matrix $\mathbf{H}_v$ is now:

$$\mathbf{H}_v = \begin{bmatrix} h_{11} & h_{12} & h_{13} & h_{14} \\ h_{12}^* & -h_{11}^* & h_{14}^* & -h_{13}^* \\ h_{21} & h_{22} & h_{23} & h_{24} \\ h_{22}^* & -h_{21}^* & h_{24}^* & -h_{23}^* \end{bmatrix} \tag{23}$$

For diagonalizing the corresponding Grammian matrix $\mathbf{G}_v = \mathbf{H}_v^H \mathbf{H}_v$, the following unitary matrix $\mathbf{V}$ is used:

$$\mathbf{V} = c \begin{bmatrix} \frac{-2Y}{Z} & \frac{-2X}{Z} & \frac{2Y}{\tilde{Z}} & \frac{2X}{\tilde{Z}} \\ \frac{-2X^*}{Z} & \frac{2Y^*}{Z} & \frac{2X^*}{\tilde{Z}} & \frac{-2Y^*}{\tilde{Z}} \\ 0 & 1 & 0 & 1 \\ 1 & 0 & 1 & 0 \end{bmatrix} \tag{24}$$

with the following abbreviations:

$$\begin{aligned} H_1 &= |h_{11}|^2 + |h_{12}|^2 + |h_{21}|^2 + |h_{22}|^2 \\ H_2 &= |h_{13}|^2 + |h_{14}|^2 + |h_{23}|^2 + |h_{24}|^2 \\ X &= h_{11}^* h_{13} + h_{14}^* h_{12} + h_{21}^* h_{23} + h_{24}^* h_{22} \\ Y &= h_{11}^* h_{14} - h_{13}^* h_{12} + h_{21}^* h_{24} - h_{23}^* h_{22} \end{aligned}$$

$$\begin{aligned} Z &= H_1 - H_2 + \sqrt{(H_1 - H_2)^2 + 4|X|^2 + 4|Y|^2} \\ \tilde{Z} &= -H_1 + H_2 + \sqrt{(H_1 - H_2)^2 + 4|X|^2 + 4|Y|^2} \\ c &= \frac{2}{\sqrt{8 + \frac{2(H_1 - H_2)^2}{|X|^2 + |Y|^2}}} \end{aligned} \tag{25}$$

With this matrix $\mathbf{V}$ the Grammian matrix $\mathbf{G}_v$ can be diagonalized and the resulting diagonal matrix $\mathbf{D} = \mathrm{diag}(\lambda_1, \lambda_2, \lambda_3, \lambda_4)$ can be calculated as:

$$\mathbf{D} = \mathbf{V}^H\,\mathbf{H}_v^H\,\mathbf{H}_v\,\mathbf{V}\,. \tag{26}$$

In our transmission scheme the transmit signal is pre-processed by $\mathbf{V}$ in order to obtain a set of four decoupled virtual channels. The factor c (25) is only necessary to normalize the total transmit power such that the SNR definition (18) still holds. The modified received signal $\tilde{\mathbf{y}}$ is filtered by $\mathbf{V}^H\,\mathbf{H}_v^H$ resulting in scaled estimates of $\mathbf{s}$:

$$\hat{\mathbf{s}} = \underbrace{\mathbf{V}^H\,\mathbf{H}_v^H\,\mathbf{H}_v\,\mathbf{V}}_{\mathbf{D}}\,\mathbf{s} + \underbrace{\mathbf{V}^H\,\mathbf{H}_v^H\,\tilde{\mathbf{n}}}_{\mathbf{n}_m}$$

Applying this scheme, now the pre-processing matrix $\mathbf{V}$ is *not* channel independent, which is in contrast to the EA scheme presented in Sec. 3. Here, the receiver has to send back some information about the channel to enable the transmitter to pre-process its signal vector

s. The entire processing (at transmitter and receiver) yields $n_T = 4$ independent virtual channels with the channel gains:

$$\lambda_1 = \lambda_2 = c^2 \left[\frac{4H_1(|X|^2+|Y|^2)}{Z^2} - \frac{4(|X|^2+|Y|^2)}{Z} + H_2 \right]$$

$$\lambda_3 = \lambda_4 = c^2 \left[\frac{4H_1(|X|^2+|Y|^2)}{\tilde{Z}^2} + \frac{4(|X|^2+|Y|^2)}{\tilde{Z}} + H_2 \right]$$

Note that one pair of the Eigenvalues is zero, if not enough receive antennas are used (e.g. in case of $n_R = 1$). The modified noise $\mathbf{n}_m$ remains uncorrelated as in the case of the EA scheme.

4.1.2 Other values of n_R

Our diagonalization method can be generalized for arbitrary values n_R. The resulting Grammian matrix $\mathbf{G}_v = \mathbf{H}_v^H \mathbf{H}_v$ has the same structure as above and therefore the same matrix $\mathbf{V}$ can be used for the pre- and post signal processing. Most equations of Sec. 4.1.1 remain unchanged. Only the following parameters used above change into:

$$H_1 = \sum_{i=1}^{n_R} \left(|h_{i1}|^2 + |h_{i2}|^2 \right)$$

$$H_2 = \sum_{i=1}^{n_R} \left(|h_{i3}|^2 + |h_{i4}|^2 \right)$$

$$X = \sum_{i=1}^{n_R} (h_{i1}^* h_{i3} + h_{i4}^* h_{i2})$$

$$Y = \sum_{i=1}^{n_R} (h_{i1}^* h_{i4} - h_{i3}^* h_{i2})$$

The difficulty with this scheme is that feedback information is already necessary to diagonalize the MIMO channel. The necessary feedback information consists of the two real-valued parameters H_1 and H_2 and the two complex-valued parameters X and Y. The benefit of this scheme is that the symbol-rate is doubled compared to the EA scheme.

The adaptive modulation algorithm operates as explained in Sec. 3.2.

The block structure of this transmission scheme is the same as for the scheme presented in Sec. 3 shown in Fig. 3.

4.2 Simulation Results

The simulations were performed with the same parameters used to analyse the EA scheme. A summary of these parameters: Simulations were done for MIMO channels with $n_T = n_R = 4$ and for several values of mean SNR. Different spatially correlated MIMO channels have been investigated. As mentioned in Sec. 2, three different spatially correlated channel types (uncorrelated, low correlation and high correlation) have been considered. Note that the simulations assume perfect channel knowledge at the receiver and error free transmission of the feedback information.

4.2.1 Mean Rate $\overline{R}$

In Fig. 7, the mean information bit rate $\overline{R}$ versus the mean SNR is shown under several conditions of spatial channel correlation for a mean BER of 10^{-3}. For this D-STTD transmission scheme still higher mean

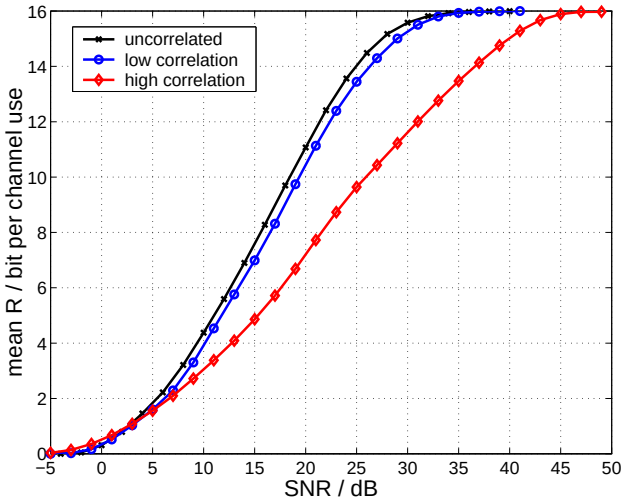

Fig. 7. Mean information bit rate $\overline{R}$ versus the mean SNR for several spatial correlation conditions (uncorrelated, low-, high-correlation) for a mean BER of 10^{-3}; D-STTD scheme; $n_T = n_R = 4$.

information rates R are achieved than in case of the EA scheme (see Fig.4). The slope of the R-curve for uncorrelated channels is approximately doubled (7 bit/10dB SNR) compared to the EA scheme. Note, that the robustness against spatial correlation is not as pronounced as for the EA scheme with its low feedback rate.

In this case the decorrelation of the channel is not as good as for the EA scheme (Fig. 8) and therefore a more severe performance degradation with respect to the mean bit rate in case of high spatial correlation is observed. Note that due to the special structure of $\mathbf{H}_v^H \mathbf{H}_v$, the virtual correlation matrix $\mathbf{R}_T^v$ still has zero correlation between the following antenna elements (i,j): (1,2), (2,1), (3,4) and (4,3).

4.2.2 Outage rate R_{out}

In Fig. 9, the CDF of the bit rate is shown for an SNR=14dB for the three spatial correlation types for a mean BER of 10^{-3}. In contrast to the scheme utilizing the EA code (Sec. 3), here the spatial correlation deteriorates the mean information rate considerably. Surprisingly, the CDFs in Fig. 9 for correlated channels are roughly only horizontally shifted versions of the CDF of the uncorrelated channel and therefore the loss in outage rate due to spatial correlation is almost the same as the loss in the mean information rate for all cases.

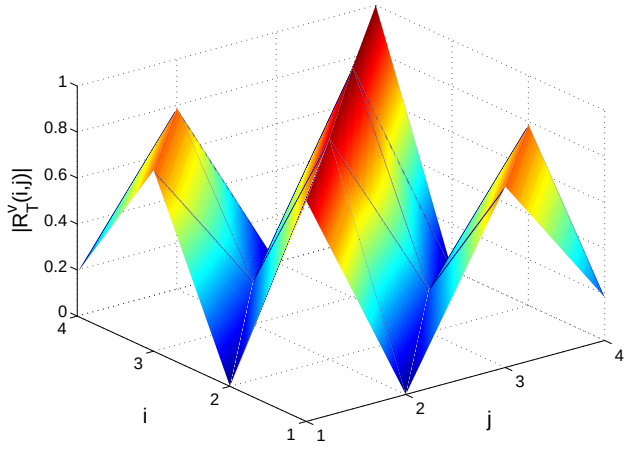

Fig. 8. Transmitter correlation $\mathbf{R}_T^v(i,j) = E_{\mathbf{H}}\left\{\mathbf{h}_{v_i}^H \mathbf{h}_{v_j}\right\}$ of the virtual channel matrix $\mathbf{H}_v = [\mathbf{h}_{v_1}\ \mathbf{h}_{v_2} \ldots\ \mathbf{h}_{v_{n_T}}]$ for the D-STTD scheme with $n_R = n_T = 4$ in case of "high spatial correlation".

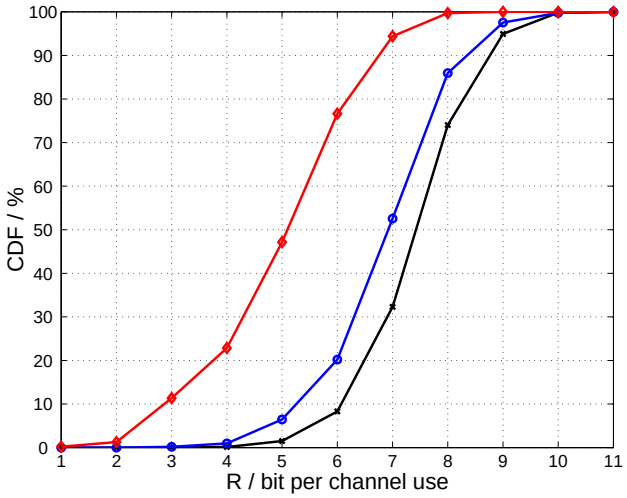

Fig. 9. CDFs of the rate R for SNR=14dB and several spatial correlation conditions (uncorrelated, low-, high-correlation) for a mean BER of 10^{-3}; D-STTD scheme; $n_T = n_R = 4$.

5 Summary and Conclusions

Two high rate closed loop MIMO transmission schemes with partial feedback have been investigated. Both systems are based on the diagonalization of the MIMO channel resulting in n_T independent virtual channels with different gains. This approach allows a ML detection with very low complexity and an independent adaptive modulation on all virtual channels. The scheme with low feedback rate based on the EA code achieves moderate to high information rate R requiring only scarce feedback information. Its mean throughput is extremely robust against spatial channel correlation. On the other hand, the D-STTD code based transmission scheme using moderate feedback information achieves a still higher information rate. However, the robustness against spatial correlation is lower than in the case of the EA scheme.

Acknowledgment

The authors would like to thank Prof. Ernst Bonek for support and encouragement and the anonymous reviewers for valuable suggestions to improve the quality of this paper.

References

[1] J.P.Kermoal, L.Schumacher, K.I.Pedersen, P.E.Mogensen, F.Frederiksen. *A Stochastic MIMO Radio Channel Model With Experimental Validation*. IEEE Journal on Selected Areas in Communications, Vol. 20, No. 6, pp. 1211-1226, August 2002.

[2] H.Özcelik, M.Herdin, W.Weichselberger, J.Wallace, E.Bonek. *Deficiencies of the Kronecker MIMO radio channel model*. Electronic Letters, vol.39, pp.1209-1210, 2003.

[3] Texas Instruments. *Double-STTD scheme for HSDPA systems with four transmit antennas: Link Level Simulation Results*. Temporary document 21(01)-0701, Release 5 Ad hoc, 3GPP TSG RAN WG1, June 2001.

[4] M.Rupp, C.F.Mecklenbräuker. *On Extended Alamouti Schemes for Space-Time Coding*. WPMC, Honolulu, pp. 115-118, Oct. 2002.

[5] B.Badic, M.Rupp, H.Weinrichter. *Adaptive Channel Dependent Extended Alamouti Space Time Code using minimum Feedback*. CIC, Seoul, Korea, Oct. 2003.

[6] H.Özcelik, M.Herdin, R.Prestros, E.Bonek. *How MIMO capacity is linked with single element fading statistics*. International Conference on Electromagnetics in Advanced Applications, Torino, Italy, pp. 775-778, 8. - 12. Sept. 2003.

[7] G.Gritsch, H.Weinrichter. *Adaptive Subspace Modulation in Spatially Correlated MIMO Systems*. PIMRC, vol. 4, pp. 1772-1776, Sep. 2002.

[8] John G. Proakis. *Digital Communications*. 3rd ed. McGraw-Hill, Inc. 1995.